Desalination and Water Treatment
www.deswater.com

doi: 10.5004/dwt.2023.30037

314 (2023) 322–329
December

Underwater remotely operated vehicle control system with optimized PID based on improved particle swarm optimization

Weixing Liu[a,b,†], Zihan Xia[a,*], Linyan Wu[a], Guangkuo Guo[c], Cheng Zhu[d], Zhiyang Zhang[a,b,*], Lin Cui[e,†]

[a]*School of Ocean Engineering, Jiangsu Ocean University, Lianyungang 222005, China, emails: jshmxzh369@163.com (Z. Xia), zhangzhiyang0530@126.com (Z. Zhang)*
[b]*Makarov College of Marine Engineering, Jiangsu Ocean University, Lianyungang 222005, China*
[c]*The Fifth Research Institute of Electronics, Ministry of Industry and Information Technology, Guangzhou 510000, China*
[d]*Science and Technology on Underwater Vehicle Laboratory, Harbin Engineering University, Harbin 150001, China*
[e]*National Ocean Technology Centre, Tianjin 300112, China*

Received 30 November 2022; Accepted 9 September 2023

ABSTRACT

On account of the exponential development of control theory and artificial intelligence technology in recent years, more and more control theory is applied to the control of robots, but PID control method due to the simple structure and good stability still has research value, the core and the difficulty is the optimization of PID parameters. In order to solve the underwater remotely operated vehicle (ROV) with high nonlinearity and strong coupling characteristics, it can adjust its attitude in time to ensure its control performance in the face of the disturbance of the external complex environment. By improving the particle swarm inertia weights, the particle swarm optimization (PSO) algorithm reduces the situation of falling into the local optimal solution and applies it to the PID adaptive parameterization. Comparing the improved PSO-PID with the traditional PID simulation, it is concluded that the improved PSO-PID control has certain improvement on the control performance of the ROV, which has certain feasibility.

Keywords: Remotely operated vehicle; PID control; Particle swarm optimization algorithm

1. Introduction

As modern control theory has developed by leaps and bounds over the past two decades, the application of underwater robots in rivers, lakes, oceans and other underwater operations is becoming more and more widespread, in which the remotely operated vehicle (ROV), because of its small size, high flexibility, and ability to transmit data in real time, since its inception in the 1950s, ROV has been widely used in a variety of underwater operations where human safety cannot be ensured. For example, nowadays, because the over-reliance on fossil fuels has caused environmental pollution and may contribute to a global energy crisis in the next few years, we have to focus on the construction of clean energy at sea [1], but in the face of the complex marine environment, in order to ensure the safety of the staff, have to be in the use of ROVs to conduct environmental exploration and equipment maintenance. In the face of such a complex natural environment and the nonlinear and time-varying characteristics of ROV underwater motion, and at the same time to improve the operational efficiency of ROV, which puts forward higher requirements for the control algorithm of ROV. A large number of research scholars at home and abroad have studied the control of

* Corresponding authors.
† These authors contribute equally to this paper and should be considered as co-first author.

ROV. Literature [2] proposes a fuzzy PID-based control and achieves good simulation results, and literature [3] is based on genetic algorithm to optimize the PID control parameters, through the essence of the genetic algorithm "survival of the fittest" to optimize the PID parameters, and achieves excellent simulation results. There are also many controls based on the traditional PID, because of its simple structure, good stability, robustness, and there is a mature Z-N method in parameter optimization, but many still rely on the engineering experience of the experts, and often after many times of adjusting the parameters may not necessarily achieve the best parameters, and is prone to overshoot or collapse, which has a great impact on the stability of the ROV control system. This has a great impact on the stability of ROV control. In this paper, from improving the stability of ROV control system, the deviation of heading motion and lateral motion of ROV are taken as two optimization objectives. Firstly, the motion transfer function is calculated and the transfer function PID control of ROV is designed, and then the improved PSO algorithm is applied to the PID to design the ROV control system, and the control effect of the two is compared through MATLAB/Simulink simulation, and it is concluded that the latter has better performance indexes and achieves a good control effect.

2. Kinematic model of the ROV

Determination of the ROV's motion pattern underwater requires analysis of the ROV's movement attitude and its spatial position. Therefore, from a mathematical modeling perspective, two coordinate systems need to be established. The former is earth-fixed frame and the latter is body-fixed frame, as shown in Fig. 1, which make up a 3D space coordinate system to calculate the nonlinear dynamics of the ROV in the next section [4].

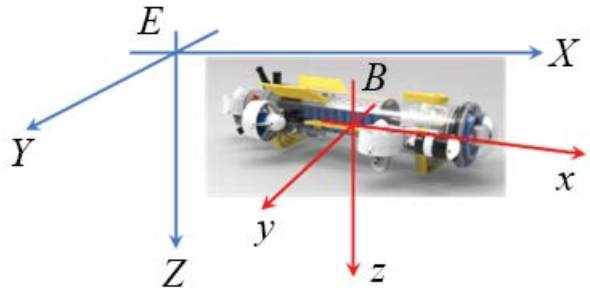

Fig. 1. Coordinate systems for a remotely operated vehicle.

The earth-fixed coordinate system E - XYZ (fixed system) is the reference system for the spatial motion of the ROV. The origin E is a point in the world, The EX-axis is in the horizontal plane and indicates the forward or backward direction of the ROV motion; the EY-axis is perpendicular to the EX-axis in the horizontal plane, representing the left and right translation of the ROV. The last EZ-axis which determines the up and down movement of the ROV is perpendicular to both EX and EY in space. The E - XYZ coordinate system constitutes a right-handed coordinate system.

The body-fixed coordinate system B - xyz (kinematic system) is fixed to the vehicle itself and moves with it. In general, the origin B is taken on the ROV's center of gravity. The horizontal Bx-axis is parallel to the side panels and points to the front end of the body, then the By-axis, perpendicular to the side plate and points to the right side of the cabin. In the end, the Bz-axis points towards the bottom of the robot. The B - xyz coordinate system also constitutes a right-handed coordinate system.

During the motion of the ROV in space, the three positions x, y, and z in the earth-fixed coordinate system, as well as the three attitude angles φ, θ, ψ with the motion of the ROV. Therefore, the establishment of the ROV motion equation in an earth-fixed coordinate system is dearly essential. To derive the equation of motion for an ROV in such a coordinate system, the motion parameters of ROV in the body fixed coordinate system must be converted to the earth-fixed coordinate system [5]. Additionally, since an ROV's movement in water involves six degrees of freedom (three linear velocities u, v, w and three angular velocities p, q, r), these variables need to be introduced for solving the equation of motion, as shown in Table 1.

The conversion from the earth-fixed coordinate system of the ROV to its body-fixed coordinate system, as mentioned earlier, can be mathematically expressed as follows:

$$\begin{bmatrix} \dot{x} \\ \dot{y} \\ \dot{z} \\ \dot{\phi} \\ \dot{\theta} \\ \dot{\psi} \end{bmatrix} = T \begin{bmatrix} x \\ y \\ z \\ p \\ q \\ r \end{bmatrix} \tag{1}$$

where T is formed as:

$$T = \begin{bmatrix} T_1 & 0^{3*3} \\ 0^{3*3} & T_2 \end{bmatrix} \tag{2}$$

In Eq. (2) one has:

$$T_1 = \begin{bmatrix} \cos\psi\cos\theta & -\sin\psi\cos\phi + \cos\psi\sin\theta\sin\phi & \sin\psi\sin\phi + \cos\psi\cos\phi\sin\theta \\ \sin\psi\cos\theta & \cos\psi\cos\phi + \sin\psi\sin\theta\sin\phi & -\cos\psi\sin\phi + \sin\psi\cos\phi\sin\theta \\ -\sin\theta & \cos\theta\sin\phi & \cos\theta\cos\phi \end{bmatrix} \tag{3}$$

$$T_2 = \begin{bmatrix} 1 & \sin\phi\tan\theta & \cos\phi\tan\theta \\ 0 & \cos\phi & -\sin\phi \\ 0 & \sin\phi/\cos\theta & \cos\phi/\cos\theta \end{bmatrix} \tag{4}$$

In general, the ROV is modeled with strongly coupled nonlinearities, and in order to reduce the experimental and computational complexity, the motion of the ROV is decomposed into two relatively decoupled sub-motions, the horizontal plane motion and the vertical plane motion.

Furthermore, when discussing horizontal movement, it is essential to consider changes in the ROV's orientation and propulsion direction while disregarding any vertical shifts in center of gravity under preset conditions. When addressing vertical movement, only alterations in depth and pitch angle should be taken into account without considering forces along the horizontal axis.

3. Dynamic model of the ROV

The movement of underwater robots in water is incredibly intricate, thus necessitating a comprehensive study of the kinematic laws governing the ROV to establish a dependable theoretical foundation for ensuring the reliable and steady operation of the whole system. Since the ROV does not need to be particularly fast in engineering operations, the role of the Kohl's force can be ignored; the ROV studied in this paper mainly has the motion of forward and backward, upward and downward, transverse roll and pitch [6], in order to facilitate the computational simulation, so its motion can be decomposed into a simple single-degree-of-freedom motion, so as to simplify the mathematical model, and in the idealization of ignoring the absence of interactions between the individual degrees of freedom The role of; based on the above force analysis, the coordinate system origin O is taken at the center of gravity of the ROV [7], as shown in Fig. 2, and thus the dynamics model is further simplified as:

$$M\dot{v} + D(v)v + g(\eta) + F_T = \tau \tag{5}$$

3.1. ROV attitude control system transfer function

Based on the equations of motion in the literature, it is known that the ROV motion system [8] is characterized by strong coupling, and the control of the ROV is mainly based on the control of the thruster, which is a typical nonlinear system, which causes a series of problems in the study of ROV motion. Therefore, deriving a reliable transfer function is crucial for the system stability performance and improving the reliability of practical experiments.

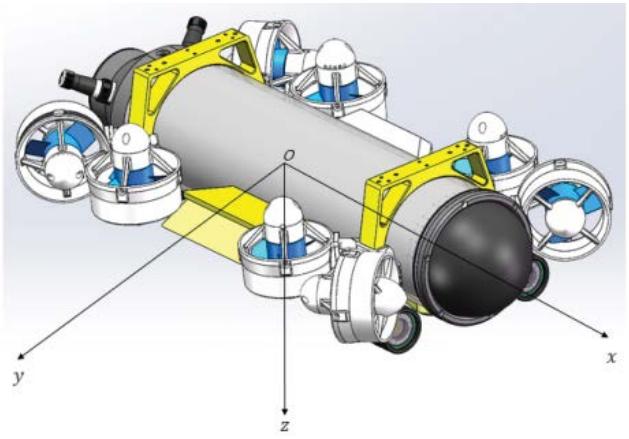

Fig. 2. Dynamic model for a remotely operated vehicle.

3.1.1. Propulsion system transfer function

In motion control studies, the ROV thruster motor [9] can be simplified as an inertial link with a transfer function of:

$$G_{K^{(S)}} = \frac{K_M}{\left(1 + T_{M^S}\right)} \tag{6}$$

where K_M is the transfer coefficient of the motor and T_M is the motor mechanical time constant [10]. For the convenience of subsequent modeling and simulation, in dealing with the nonlinear propulsion is to linearize the propulsion is treated with the expression:

$$T = Cn \tag{7}$$

$$C = 2K_T \rho D^4 n_0 \tag{8}$$

where K_T is the coefficient of the thruster; n_0 is the motor speed. From this, the thruster transfer function is derived as:

$$G_{p^{(s)}} = C \tag{9}$$

Through actual measurements and calculations, as well as reading the relevant literature, the system transfer function can be introduced as:

$$G_{M^{(s)}} = \frac{0.5}{\left(1 + 1.8S\right)} \tag{10}$$

3.1.2. Motion system transfer function

(1) Heading motion model: When the ROV only changes course, that is, completes the fixed-point steering motion in the horizontal plane [11], and the position of the center of gravity does not change, at this time, its equation of motion is as follows:

$$\left(I_Z - N_r\right)r = N_r r + N_p \tag{11}$$

After Laplace transformation, the transfer function can be obtained:

$$G_{\psi^{(S)}} = \frac{1}{\left(I_Z - N_r\right)s^2 - N_r s} \tag{12}$$

(2) Lateral motion model: When the ROV does lateral motion, transverse and longitudinal motion is not involved, and its center of gravity position does not change. In this case, the motion equation is as follows:

$$G_{\varphi^{(S)}} = \frac{1}{\left(I_x - K_p\right)s^2 - K_p s} \tag{13}$$

After measurements and Solidworks modeling calculations [12] the relevant data of the ROV are shown in Table 2.

The open-loop transfer function of the ROV system [13] can be obtained by combining the motion transfer

function of the ROV with the motor transfer function, where the heading motion transfer function is:

$$G_{\psi C^{(s)}} = G_{M^{(s)}} G_{\psi^{(s)}} = \frac{0.5}{1.54s^3 + 3.59s^2 + 1.52s} \tag{14}$$

The lateral motion transfer function is:

$$G_{\varphi C^{(s)}} = G_{M^{(s)}} G_{\varphi^{(s)}} = \frac{0.5}{5.26s^3 + 4s^2 + 0.6s} \tag{15}$$

4. Improvement of PSO-PID control

4.1. Conventional PID control

The three links of proportional (P), integral (I) and derivative (D) are connected to form a proportional integral differential controller, referred to as PID controller [14], and its working principle is shown in Fig. 3.

From Fig. 3:

$$e(t) = r(t) - y(t) \tag{16}$$

Thus, the relationship between $e(t)$ and $u(t)$ is obtained:

$$u(t) = K_p e(t) + K_i \int_0^t e(\tau) d(\tau) + K_d \frac{de(t)}{dt} \tag{17}$$

where K_p, K_d and K_i correspond to the coefficients of the above three control links, respectively. The selection and adjustment of these three coefficients are crucial for the safety and stability performance of the whole system. However, they are often adjusted by expert engineering experience, which is often time-consuming and labor-intensive, so in the following section, a PID based on improved PSO with adaptive performance is introduced.

Table 1
Velocity parameters

Vector	X	Y	Z
Linear velocity	u	v	w
Angular velocity	p	q	r

4.2. Improvement of PSO algorithm

The PSO algorithm represents an evolutionary computing technology, belongs to the adaptive optimization algorithm of population search, proposed by Dr. Eberhart and Dr. Kennedy in 1995. The algorithm is derived from the study of foraging behavior in bird flocks, and has rapidly evolved into a famous evolutionary algorithm over the past few decades. This algorithm is similar to genetic algorithm (GA) than and, starting from a random solution, search for the optimal solution through iteration; finally, through the PSO algorithm is similar to genetic algorithm [15], it begins with random number and finds the optimal result after iteration; in the end of calculation, it determines whether the data is acceptable by fitness. Compared to GA, the former reduces the need for crossover and mutation operations while tracking the optimal solution at present time in order to search for global optima [16]. PSO algorithm, which is easy to grasp, has high accuracy and fast convergence, so it is extensively applied to the control system, and its workflow as shown in Fig. 4.

Table 2
Remotely operated vehicle-related raw data

m (kg)	10
L (m)	0.65
I_x	2.8
I_Z	0.79
K_p	–0.6
k_p	–0.12
N_r	–1.52
N_r	–0.065

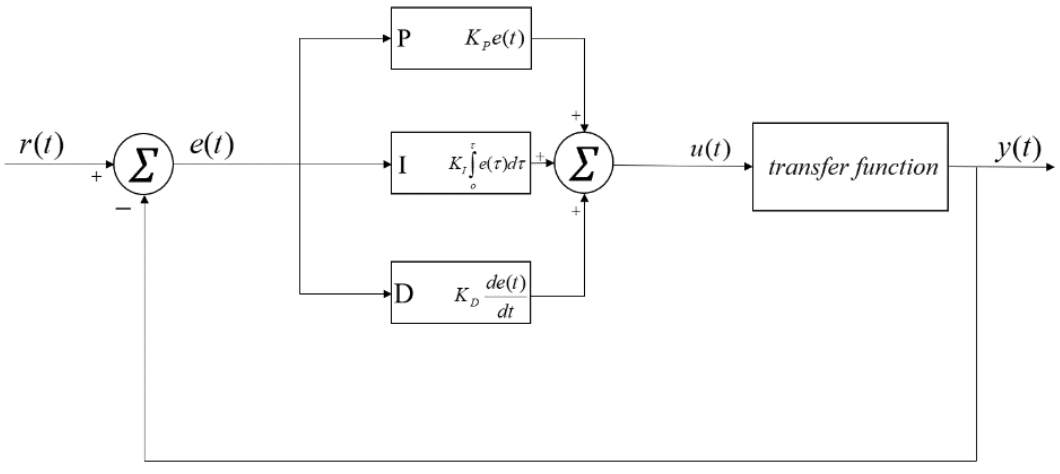

Fig. 3. Block diagram of conventional PID.

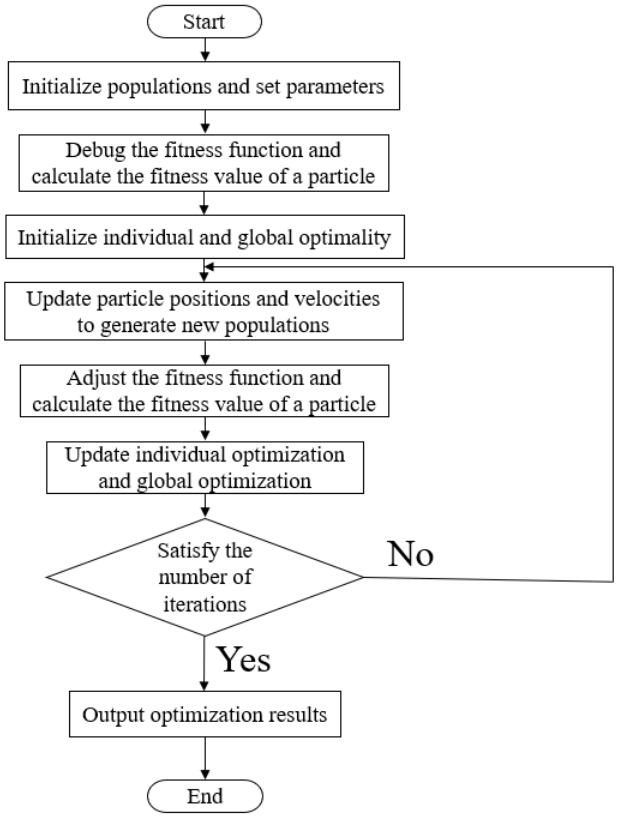

Fig. 4. Flowchart of the PSO algorithm.

The whole process of particle swarm optimization search is to initialize the information of the initial particles in the particle swarm, after that carry out the iterative process of the whole algorithm, in which the adaptation degree of particles during each iteration is calculated, and according to the adaptation degree, the particles carry out the updating of the velocity and position information until the end of the iteration. At the end of the iteration, the globally optimal particle is obtained, and the parameter combination of the controller also reaches the optimum under the preset conditions, so as to improve the control ability of the controller.

From the references and related materials, the inertia weight, denoted by ω, represents the ability of particle's capacity to retain its previous velocity, the larger ω is, the fewer iterations can reduce the number of iterations, which is favorable to detach the local minimum and facilitates the global search, as well as the smaller ω is beneficial to the accurate local search of the current search area, which makes the algorithm converge, but ω is too large and easy to cause the phenomenon of convergence and oscillation of the optimal solution too soon [17], so the inertia weight has a great influence on the optimization process of the algorithm. ω exerts a significant impact on the optimization process of the algorithm, so in this paper, we introduce the liner decreasing inertia weight (LDIW), which was firstly proposed by Wang et al. [18], that is:

$$\omega = \omega_{start}\left(\omega_{start} - \omega_{end}\right)\frac{T_{max} - k}{T_{max}} \tag{18}$$

where the ω_{start} is the initial inertia weight, at the maximum number of iterations, ω_{end} represents the inertia weight, k is the current number of iterations, T_{max} is the maximum number of iterations, through the literature, it can be obtained that ω_{start} takes 0.9, ω_{end} takes 0.4 when the best results.

By utilizing the optimization features of the PSO algorithm, the three parameters of the PID controller are adjusted, and the dimension of the PSO algorithm is set to 3, and the decomposition amount of each particle's position information in these 3 dimensions corresponds to a set of PID parameter values [19]. The block diagram of the system is shown in Fig. 5.

The particle dimension in the experiment is set to 3, that is, K_p, K_i, K_d. In order to avoid the blind search of particles in the algorithm, the upper and lower limits of the position and step size are usually set according to the specific dare of the control volume in the last century [$-X_{max}$, X_{max}],

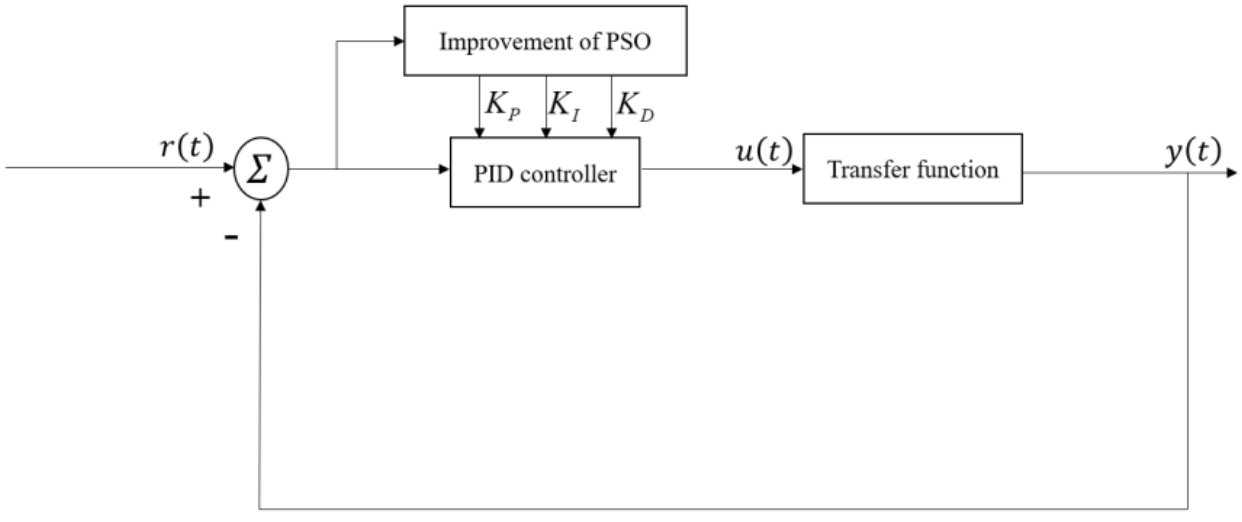

Fig. 5. Improvement of PSO-PID system control principal block diagram.

$[-V_{max}, V_{max}]$, in which the updating formulas of the particle position and step size are:

$$v_{id}^{k+1} = w \times v_{id}^{k} + c_1 \times r_1 \times \left(p_{id} - x_{id}^{k}\right) + c_2 \times r_2 \times \left(p_{gd} - x_{id}^{k}\right) \tag{19}$$

$$x_{id}^{k+1} = x_{id}^{k} + v_{id}^{k+1} \tag{20}$$

where v_{id}^{k+1} represents the velocity information of the i-th particle on the d dimension in the k+1 iteration, x_{id}^{k+1} represents the position information of the i-th particle on the d dimension in the k+1 iteration, c_1 is the local learning factor and c_2 the global learning factor, is usually set to 2 and ω is the inertia weight.

In evaluating the merits and disadvantages of the desired values, the fitness function is introduced. So far, the most comprehensive and reasonable fitness value function is ITEA method [20], namely:

$$J = \int_0^{\infty} t\left|e(t)\right| dt \tag{21}$$

The improved PSO-PID control flow is shown in Fig. 6.

5. Simulation results

The parameter values of the improved PSO algorithm are set as follows: the population size is set to 100, the learning factors C_1 and C_2 are taken as 2, the dimension is taken as 3 because the control of the three parameters P, I and D is targeted, the number of iterations is 50 and the minimum adaptation value is 0.01.

According to the above to establish the ROV system model, Simulink in MATLAB is used to complete the system construction, and the improved PSO algorithm is written into the PID control to debug and then simulated. Compare the improved PSO-PID and traditional PID, analyze the

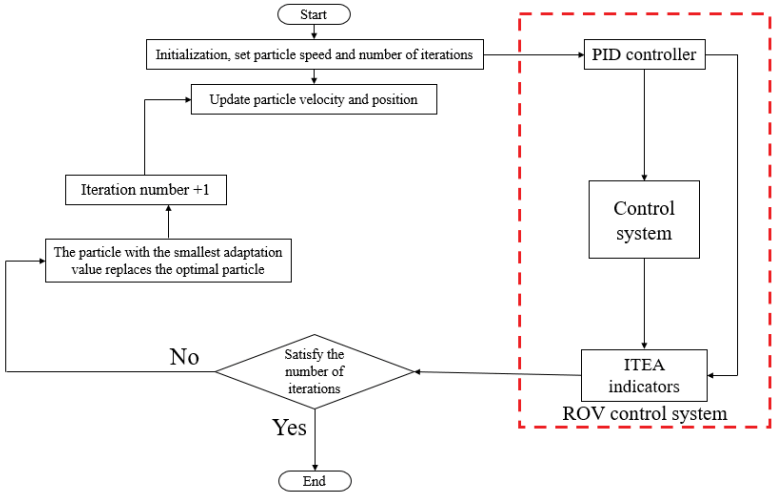

Fig. 6. Improved PSO-PID control flowchart.

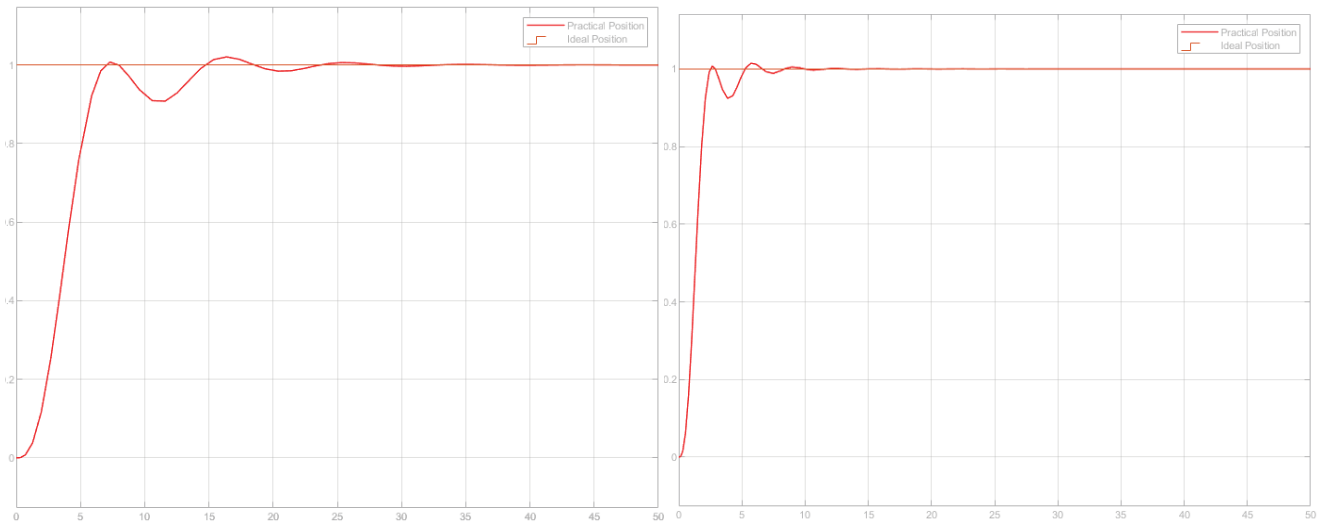

Fig. 7. Heading and lateral motion simulation curve.

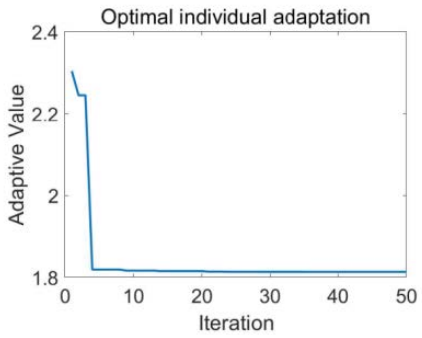

Fig. 8. Number of iterations and adaptation values.

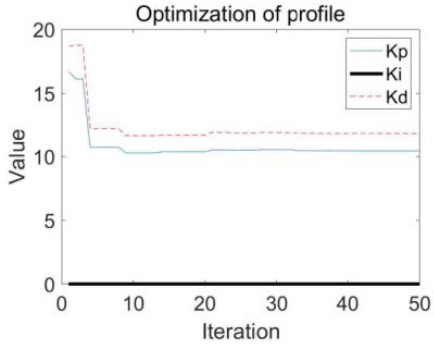

Fig. 9. PID parameter value.

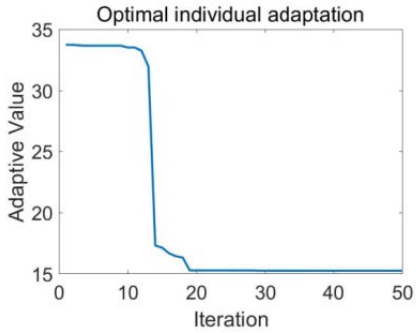

Fig. 10. Number of iterations and adaptation values.

advantages and shortcomings of each system, and continue to optimize. The ideal output signals are set to 1 and sampled for 50 s, and the heading motion and lateral motion samples are shown in Fig. 7.

The number of iterations of the heading motion with PID parameters are shown in Figs. 8 and 9.

The number of iterations of lateral motion with PID parameters are shown in Figs. 10 and 11.

The simulation of the traditional PID control for heading motion and lateral motion is shown in Figs. 12 and 13, compared with which the improved PSO-PID control has better stability performance for the whole motion system, although it is slightly slower than the traditional PID in terms of the response speed, but it does not have the obvious overshooting phenomenon of the traditional PID.

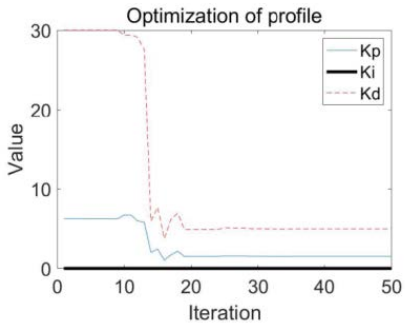

Fig. 11. PID parameter value.

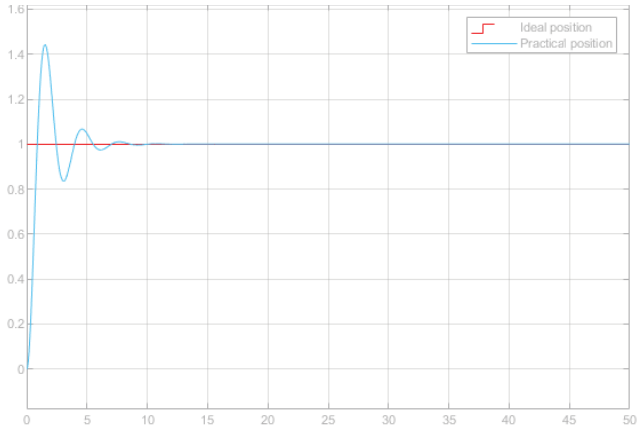

Fig. 12. Simulation of conventional PID control for heading motion.

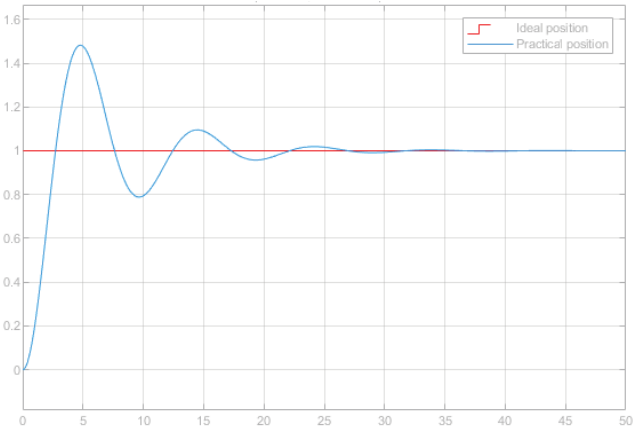

Fig. 13. Simulation of conventional PID control for lateral motion.

6. Conclusion

This paper takes the attitude control of ROV as the core, improves the inertia weight which is generally set to be fixed in PSO algorithm to liner decreasing inertia weight, takes the improvement of PSO algorithm in PID parameter control of motion as the design purpose, and utilizes MATLAB to carry out the simulation, and tests the control performances of the heading motion and the lateral motion,

respectively. The experimental data show that the improved PSO algorithm effectively improves PID parameter tuning process with high accuracy, which can effectively improve the control efficiency without the overshooting phenomenon of the traditional PID, which verifies the effectiveness and superiority of the algorithm applied in the ROV motion control. Further research work is for the faster response speed and higher stability performance of the system, as well as the combination with other optimization algorithms (such as ant colony algorithm [21], neural network algorithm [16], etc.) to achieve a better motion control effect, and a comparative analysis.

Acknowledgment

This paper was supported by National Natural Science Foundation of China (Nos. 52001138; 52071094), Natural Science Foundation of Jiangsu Province (Nos. BK20201029; 21kjb580011) and Key Research and Development Plan of Lianyungang City (Nos. CG2224).

References

[1] Z. Zhang, X. Chen, H. Wu, W. Liu, L. Cui, Numerical study of a novel hybrid system with the Wavestar wave energy converter array and a SPIC semi-submersible floating platform, J. Cleaner Prod., 407 (2023) 137178, doi: 10.1016/j.jclepro.2023.137178.
[2] M. Dong, J. Li, W. Chou, Depth control of ROV in nuclear power plant based on fuzzy PID and dynamics compensation, Microsyst. Technol., 26 (2020) 811–821.
[3] J. Xu, N. Wang, Optimization of ROV Control Based on Genetic Algorithm, 2018 OCEANS-MTS/IEEE Kobe Techno-Oceans (OTO), Kobe, Japan, 28–31 May 2018.
[4] G. Antonelli, On the use of adaptive/integral actions for six-degrees-of-freedom control of autonomous underwater vehicles, IEEE J. Oceanic Eng., 32 (2007) 300–312.
[5] B.H. Jun, H.W. Shim, P.M. Lee, H. Baek, S.K. Cho, D.J. Kim, Workspace control system of underwater tele-operated manipulators on ROVs, Ocean Eng., 37 (2010) 1036–1047.
[6] F.R. Driscoll, R.G. Lueck, M. Nahon, Development and validation of a lumped-mass dynamics model of a deep-sea ROV system, Appl. Ocean Res., 22 (2000) 169–182.
[7] A. Hammoud, J. Sahili, M. Madi, E. Maalouf, Design and dynamic modeling of ROVs: estimating the damping and added mass parameters, Ocean Eng., 239 (2021) 109818, doi: 10.1016/j.oceaneng.2021.109818.
[8] F. Dukan, ROV Motion Control Systems, Skipnes Kommunikasjon As, Travbanevegen 6, Trondheim, Norway, 2014.
[9] M.S. Mohd Aras, S.S. Abdullah, A.A. Rahman, M.A.A. Aziz, Thruster modelling for underwater vehicle using system identification method, Int. J. Adv. Rob. Syst., 10 (2013) 252, doi: 10.5772/56432.
[10] Z. Zhang, B. Wu, L. Wu, W. Liu, L. Liu, N. Li, L. Cui, Optimization of the bionic wing shape of tidal turbines using multi-island genetic algorithm, Machines, 11 (2023) 43, doi: 10.3390/machines11010043.
[11] W. Liu, L. Liu, H. Wu, Y. Chen, X. Zheng, N. Li, Z. Zhang, Performance analysis and offshore applications of the diffuser augmented tidal turbines, Ships Offshore Struct., 18 (2023) 68–77.
[12] Z. Zhang, F.M.A. Altalbawy, M. Al-Bahrani, Y. Riadi, Regret-based multi-objective optimization of carbon capture facility in CHP-based microgrid with carbon dioxide cycling, J. Cleaner Prod., 384 (2023) 135632, doi: 10.1016/j.jclepro.2022.135632.
[13] A. Tanveer, S.M. Ahmad, Cross-coupled dynamics and MPA-optimized robust MIMO control for a compact unmanned underwater vehicle, J. Mar. Sci. Eng., 11 (2023) 1411, doi: 10.3390/jmse11071411.
[14] I. Lopez-Sanchez, J. Moreno-Valenzuela, PID control of quadrotor UAVs: a survey, Annu. Rev. Control, 56 (2023) 100900, doi: 10.1016/j.arcontrol.2023.100900.
[15] Ö. Ekrem, B. Aksoy, Trajectory planning for a 6-axis robotic arm with particle swarm optimization algorithm, Eng. Appl. Artif. Intell., 122 (2023) 106099, doi: 10.1016/j.engappai.2023.106099.
[16] X. Sun, M. Xie, F. Zhou, X. Wu, J. Fu, J. Liu, Hierarchical evolutionary construction of neural network models for an Atkinson cycle engine with double injection strategy based on the PSO-Nadam algorithm, Fuel, 333 (2023) 126531, doi: 10.1016/j.fuel.2022.126531.
[17] Y. Lin, D. Xin, X. Bian, Q. Zhang, T. Li, Improved adaptive inertia weight PSO algorithm and its application in nuclear power pipeline layout optimization, Chin. Ship Res., 18 (2023) 1–12, 25.
[18] J. Wang, X. Wang, X. Li, J. Yi, A hybrid particle swarm optimization algorithm with dynamic adjustment of inertia weight based on a new feature selection method to optimize SVM parameters, Entropy, 25 (2023) 531, doi: 10.3390/e25030531.
[19] N.H. Sahrir, M.A.M. Basri, PSO–PID controller for quadcopter UAV: index performance comparison, Arabian J. Sci. Eng., 48 (2023) 15241–15255.
[20] N. Li, Y. Su, Z. Wang, W. Liu, M. Ashraf, Z. Zhang, Hydrodynamic analysis of rigid and flexible pectoral fins, J. Environ. Biol., 37 (2016) 1105–1116.
[21] M.I. Azeez, A.M.M. Abdelhaleem, S. Elnaggar, K.A.F. Moustafa, K.R. Atia, Optimization of PID trajectory tracking controller for a 3-DOF robotic manipulator using enhanced Artificial Bee Colony algorithm, Sci. Rep., 13 (2023) 11164, doi: 10.1038/s41598-023-37895-3.